ISSN 0001-4338, Izvestiya, Atmospheric and Oceanic Physics, 2018, Vol. 54, No. 10, pp. 1460–1469. © Pleiades Publishing, Ltd., 2018.
Original Russian Text © A.A. Lyubushin, 2018, published in Geofizicheskie Protsessy i Biosfera, 2018, Vol. 17, No. 3, pp. 62–77.

Cyclic Properties of Seismic Noise and the Problem of Predictability of the Strongest Earthquakes in Japanese Islands

A. A. Lyubushin*

Schmidt Institute of Physics of the Earth, Russian Academy of Sciences, Moscow, 123995 Russia
**e-mail: lyubushin@yandex.ru*

Abstract—The results of an analysis of the properties of low-frequency seismic noise in the Japanese Islands from early 1997 to March 2018 are presented. The time interval under consideration includes one of the largest seismic disasters of recent times, the Tohoku earthquake of March 11, 2011. The presence of a dense network of seismic observations provides a unique opportunity to investigate how the preparation of a strong earthquake is reflected in changes in the properties of seismic noise in time and space. An analysis of the clustering of the daily multifractal and entropic properties of seismic noise in a 1-year moving time window averaged over all stations of the network made it possible to find a 2.5-year periodicity established since the beginning of 2003. This periodicity correlates with the occurrence of strong earthquakes in Japan. Studying features of the spatial distribution of seismic-noise properties allows us to put forward a hypothesis about the increased danger of the next megaearthquake in Japan in the area of the contact between the northern boundary of the Philippine Sea plate and Honshu Island, in the Nankai deepwater trough area, not far from Tokyo. In the Japanese Islands, in addition to the network of seismic observations, there is a dense network of fixed GPS points for which observations are available from the beginning of March 2015 with a time step of 5 min. The availability of such measurements makes it possible to complement the analysis of seismic-noise properties and to calculate the degree of correlation of GPS data at any point from measurements at neighboring stations. An analysis and processing of measurement results show that the most intense spot of increased correlation of the Earth's surface tremor, measured using GPS, is located in the Nankai Trough, with the center at the point of 34° N and 138° E.

Keywords: seismic noise, Earth's tremor, multifractals, entropy, earthquake precursors
DOI: 10.1134/S0001433818100067

INTRODUCTION

One of main difficulties in solving the problem of predicting the instant of a strong seismic event is the presence of a trigger mechanism generating the earthquake (Sobolev, 2011). The accumulation of tectonic energy in a large volume of the Earth's crust substance does not necessarily imply an energy release in the form of a sharp movement at the boundary of blocks. The appearance of a regular seismic event often needs an external shock of low energy or a trigger capable of unbalancing the system of crustal blocks and provoking an earthquake. To date, the physical nature of triggers is poorly understood and, most likely, it will never be understood completely, just due to the fact that the trigger, by definition, is an event with a low energy. If a possible earthquake does not get its trigger, the accumulated energy can dissolve in the form of a series of smooth movements, which are often called slow or quiet earthquakes.

In connection with the trigger mechanism of earthquake generation, it seems promising to develop methods allowing one to indirectly estimate the process of tectonic energy accumulation in a moving time window in a certain seismically active region. In this approach, time windows that are in correspondence with higher values of accumulated energy are interpreted as time intervals of a higher seismic hazard. The method proposed below is based on a cluster analysis of multifractal and entropic properties of waveforms of low-frequency seismic noise detected by the F-net network of broadband seismic stations in Japanese Islands.

Most attention in this paper is paid to processing the seismic-noise data obtained by the network of seismic stations in the Japanese islands. The choice of the study object was determined by the fact that one of strongest megaearthquakes in the history of instrumental seismology occurred March 11, 2011, in Japan—the 9.1-magnitude Tohoku earthquake. Japan is also a region with an extremely dense network of geophysical observation stations, data from which are freely available on the Internet. In addition to seismic data, time series of Earth's surface displacements recorded in the network of GPS stations are considered. Such a combination yields a unique possibility to verify different hypotheses on how processes of prepa-

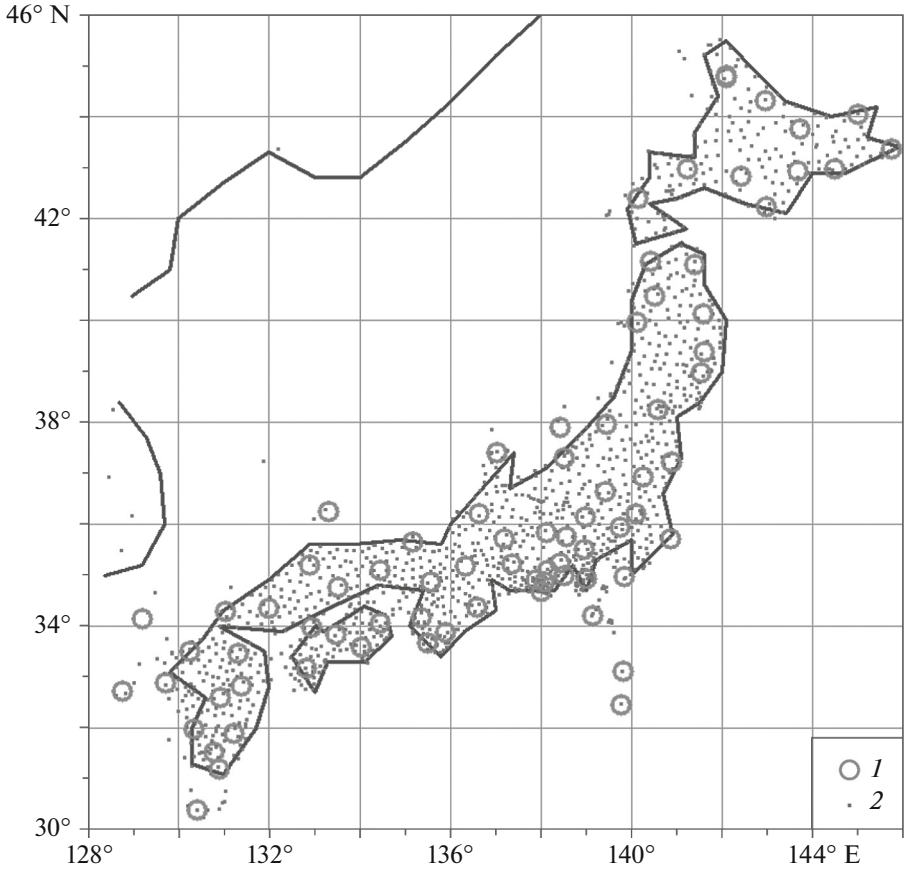

Fig. 1. Arrangement of (*1*) 78 broadband seismic stations of the F-net in Japanese islands and (*2*) 1341 stationary sites of the GPS network for measuring displacements of the Earth's surface.

rations of a seismic catastrophe and its consequences affect the statistical properties of ground vibrations.

INITIAL DATA

The seismic data are taken from the F-net broadband network in Japan. It consists of 84 stations and operates continuously beginning from 1997. Data from this network are freely available on the Internet: http://www.fnet.bosai.go.jp/top.php?LANG=en. Figure 1 shows the position of 78 F-net stations; six stations located at small remote islands south of 30° N were excluded from consideration. Data of vertical components with a sampling frequency of 1 Hz (*LHZ*-records) were selected and then reduced to a time step of 1 min by calculating mean values in successive time intervals with a length of 60 values.

SEISMIC NOISE PROPERTIES USED

Low-frequency microseismic vibrations are an important source of information about processes in the Earth's crust despite the fact that the main energy of these vibrations is caused by processes in the atmosphere and ocean: variations in the atmospheric pressure and oceanic wave impact on the shore and shelf. The Earth's crust is in fact the propagation medium for the energy from atmospheric and oceanic processes and, since transfer properties of the Earth's crust depend on its state, statistical properties of microseisms also reflect changes in properties of the lithosphere. In (Sobolev, 2014), approaches to studying the properties of seismic noise for problems of studying the Earth's dynamics and earthquake prediction were presented. Below, we use the mathematical apparatus developed in (Lyubushin, 2007–2014c, 2016) for studying the variability of seismic noise properties in time and space in estimating in a moving time window.

Let $x(t)$ be a finite sample of a random signal and $t = 1, 2, ..., N$ be the index numerating successive readings (discrete time). The normalized entropy of a finite sample is defined by the formula

$$En = -\sum_{k=1}^{N} p_k \log(p_k) \Big/ \log N\,, \quad p_k = c_k^2 \Big/ \sum_{j=1}^{N} c_j^2\,. \qquad (1)$$

Here, c_k, $k = 1, ..., N$, are coefficients of the orthogonal wavelet expansion with a certain basis.

Below, 17 orthogonal Daubechies wavelets were used: ten regular bases with a minimum support hav-

ing from one to ten vanishing moments and seven so-called Daubechies symlets (Mallat, 1998) having from four to ten vanishing moments. For each of the bases, the normalized entropy of the distribution of squared coefficients from (1) was calculated and the basis providing the minimum for the quantity (1) was found. Note that, by virtue of orthogonality of the wavelet transform, the sum of squared coefficients is equal to the variance (energy) of the signal $x(t)$. Therefore, quantity (1) calculates the entropy of the vibration energy distribution at different spatial and temporal scales. By construction, $0 \le En \le 1$. Statistic En was used in (Lyubushin, 2012a, 2013a, 2013b, 2014a, 2017; Lyubushin et al., 2015) when studying properties of seismic noise both at the regional level (Japanese Islands, Kamchatka, and California) and at the global level.

In addition to seismic-noise entropy, parameters of the multifractal singularity spectrum are also used below (Feder, 1988). Let us consider random vibration $x(t)$ on a time interval $(t - \delta/2;\ t + \delta/2)$ with length δ and center at a time point t. Consider the range $\mu(t, \delta)$ of the random vibration on this interval, i.e., the difference between the maximum and minimum values:

$$\mu(t,\delta) = \max_{t-\delta/2 \le s \le t+\delta/2} x(s) - \min_{t-\delta/2 \le s \le t+\delta/2} x(s). \qquad (2)$$

Let $\delta \to 0$; then, $\mu(t, \delta)$ also tends to zero. Here, however, the rate of this decrease is important. If the rate is determined by law $\delta^{h(t)}$: $\mu(t, \delta) \underset{\delta \to 0}{\approx} \delta^{h(t)}$ or if there exists the limit

$$h(t) = \lim_{\delta \to 0} (\log(\mu(t,\delta)) / \log \delta), \qquad (3)$$

quantity $h(t)$ is called the Hölder—Lipschitz exponent. If quantity $h(t)$ does not depend on time instant t, $h(t) = \text{const} = H$, random vibration $x(t)$ is called monofractal, and quantity H is called the Hurst exponent. If the Hölder—Lipschitz exponents $h(t)$ are different for different time instants t, the random vibration is called a multifractal and one can define the concept of singularity spectrum $F(\alpha)$ for it (Feder, 1988). For this purpose, we extract a set $C(\alpha)$ of time instants t with the same value α of the Hölder—Lipschitz exponent: $h(t) = \alpha$. Sets $C(\alpha)$ exist (i.e., contain some elements and are not empty sets) not for all values α; i.e., minimum $\alpha_{\min}$ and maximum $\alpha_{\max}$ exist so that the sets $C(\alpha)$ are nonempty only for $\alpha_{\min} < \alpha < \alpha_{\max}$. The multifractal singularity spectrum $F(\alpha)$ is the fractal dimension of the set of points $C(\alpha)$. Parameter $\Delta\alpha = \alpha_{\max} - \alpha_{\min}$, called the singularity spectrum support width, is an important multifractal characteristic. Also of considerable interest is argument α^* providing the maximum to the singularity spectrum: $F(\alpha^*) = \max_{a_{\max} \le \alpha \le \alpha_{\min}} F(\alpha)$. It is called the generalized Hurst exponent. The singularity spectrum maximum cannot exceed 1 ($0 < F(\alpha^*) \le 1$), and usually $F(\alpha^*) = 1$. For a monofractal signal, $\Delta\alpha = 0$ and $\alpha^* = H$.

Multifractal characteristics of signals are estimated below using a method based on the analysis of fluctuations after the elimination of scale-dependent trends (Kantelhardt et al., 2002). In (Lyubushin and Sobolev, 2006; Lyubushin, 2007–2014c, 2016; Lyubushin et al., 2015), multifractal parameters $\Delta\alpha$, α^*, and $\alpha_{\min}$ were used for analyzing seismic noise properties and estimating the seismic hazard by properties of this noise in Japan and in Kamchatka.

Figure 2 presents plots of medians (calculated over all stations of the F-net network) of daily noise characteristics $\Delta\alpha$, α^*, $\alpha_{\min}$, and En together with plots of their moving averages in a 57-day time window from the beginning of 1997 to March 31, 2018.

CLUSTER ANALYSIS OF SEISMIC NOISE PROPERTIES

Let $\vec{\xi}^{(t)} = (\Delta\alpha, \alpha^*, \alpha_{\min}, En)_t$ denote a four-dimensional vector of daily median values of analyzed properties of seismic noise, where $t = 1, \ldots, 7760$ is a discrete time index numerating successive days in the range from January 1, 1997, to March 31, 2018. Consider time windows with a length of 365 days (1 year) taken with a shift of 3 days and, for each time window, implement a cluster analysis of a cloud consisting of $L = 365$ four-dimensional vectors $\vec{\xi}^{(t)}$ belonging to the current time window. Before the operation of cluster analysis, we carry out normalization and winsorization (Huber, 1981) of components of the vector $\vec{\xi}^{(t)}$. Let $\xi_k^{(t)}$ be scalar components of the vector $\vec{\xi}^{(t)}$, $k = 1, \ldots, 4$, and let $\overline{\xi}_k = \frac{1}{L}\sum_{t=1}^{L} \xi_k^{(t)}$, $\sigma_k^2 = \frac{1}{L-1}\sum_{t=1}^{L} (\xi_k^{(t)} - \overline{\xi}_k)^2$ be sample estimates of the mean value and variance of each scalar component in the current time window. We implement in each window the iteration procedure of the transition from $\xi_k^{(t)}$ to the quantities $\zeta_k^{(t)} = (\xi_k^{(t)} - \overline{\xi}_k)/\sigma_k$ and cutoffs of values $\zeta_k^{(t)}$ falling outside the limits $\pm 3\sigma_k$; i.e., for each iteration, if $\zeta_k^{(t)} > 3\sigma_k$, it is set $\zeta_k^{(t)} = 3\sigma_k$, and, if $\zeta_k^{(t)} < -3\sigma_k$, then $\zeta_k^{(t)} = -3\sigma_k$. These iterations are stopped if values of these quantities $\overline{\xi}_k$ and σ_k are stabilized and become equal to $\overline{\xi}_k = 0$ and $\sigma_k = 1$. After these preliminary operations, a cloud consisting of L four-dimensional vectors $\vec{\xi}^{(t)}$ is formed in each time window.

The next step in the cluster analysis is the transition from four-dimensional vectors $\vec{\xi}^{(t)}$ to three-dimensional vectors $\vec{\psi}^{(t)}$ consisting of the first three main components (Aivazyan et al., 1989) of vectors $\vec{\zeta}^{(t)}$. For this purpose, the 4×4 covariance matrix with elements $R_{kj} = \frac{1}{L}\sum_{t=1}^{L} \zeta_k^{(t)} \zeta_j^{(t)}$, $k, j = 1, \ldots, 4$ is calculated in each

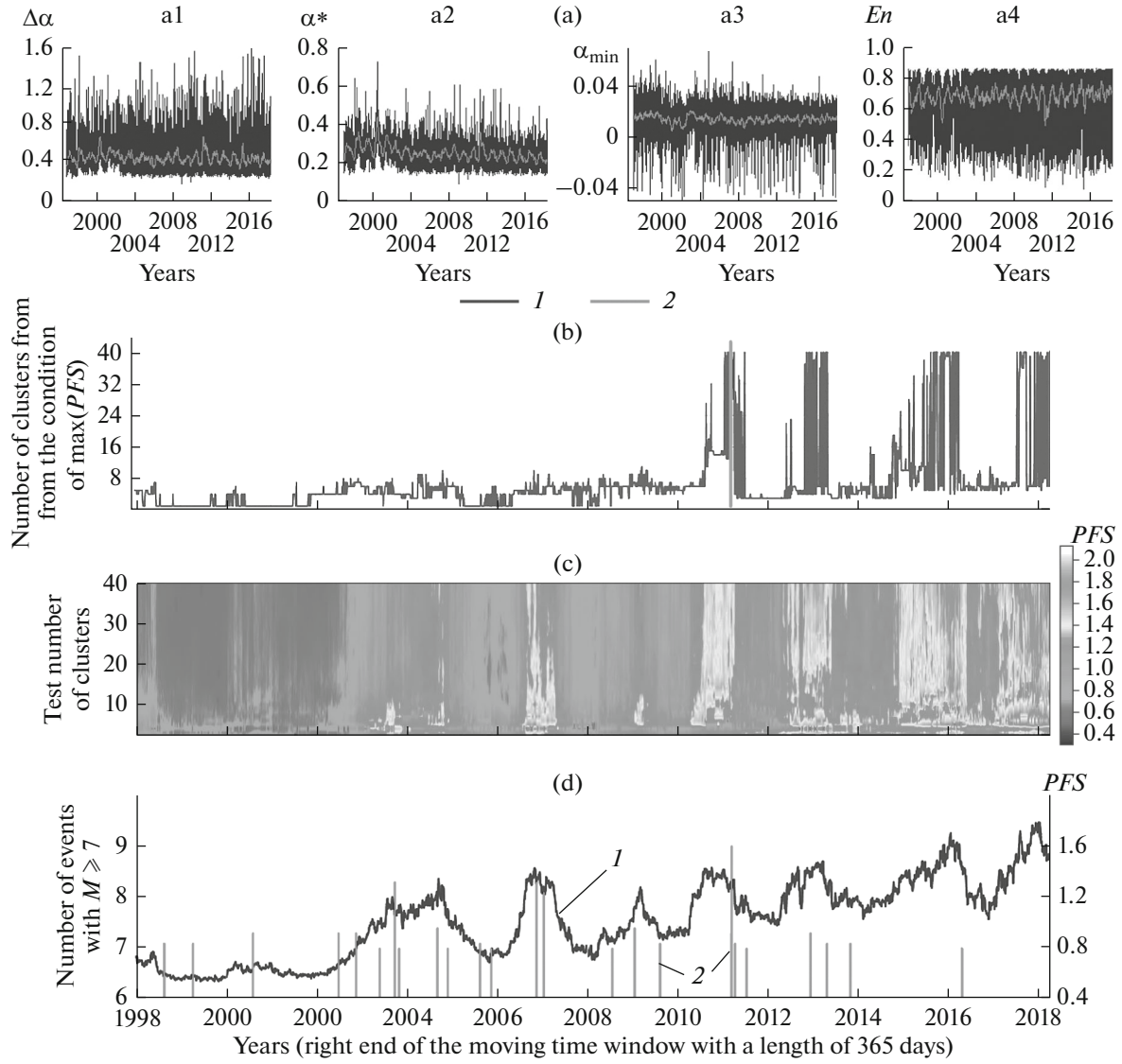

Fig. 2. (a) (*1*) Measurement of daily medians of the properties of seismic noise and (*2*) their moving averages in a 57-day window for the interval from January 1, 1997, to March 31, 2018. (b) Best number of clusters as a function of the position of the right end of the moving time window. The vertical red line shows the instant of the megaearthquake of March 11, 2011. (c) Variability diagram for the quantity *PFS* depending on the position of the right end of the time window and test number of clusters from 2 to 40. (d) (*1*) Mean value of the statistic *PFS* as a function of the position of the right end of the time window and (*2*) sequence of seismic events with magnitude $M \geq 7$ in a rectangular region with geographic coordinates (28°–48° N) × (128°–156° E).

window. Let λ_k be eigenvalues of the matrix (R_{kj}) in descending order, $\lambda_1 \geq \lambda_2 \geq \lambda_3 \geq \lambda_4$, and let (η_{kj}) be a 4×4-matrix, the columns of which are eigenvectors corresponding to the eigenvalues λ_k of the matrix (R_{kj}). Scalar components of the vector $\vec{\psi}^{(t)}$ of the first three main components are projections of vector $\vec{\zeta}^{(t)}$ onto eigenvectors of the covariance matrix (R_{kj}) corresponding to the first three maximum eigenvalues $\psi_a^{(t)} = \sum_{k=1}^{4} \eta_{ka}\, \zeta_k^{(t)}$, $a = 1, 2, 3$.

Let us divide the cloud of three-dimensional vectors $\vec{\psi}^{(t)}$ into a given test number q of clusters using the method of k-means (Duda and Hart, 1973). Let Γ_r, $r = 1, ..., q$, denote the clusters and let $\vec{z}_r = \sum_{\vec{\psi} \in \Gamma_r} \vec{\psi}/n_r$ be vectors of centers of clusters Γ_r, and n_r be the number of vectors belonging to cluster Γ_r, $\sum_{r=1}^{q} n_r = L$. The vector $\vec{\psi}^{(t)} \in \Gamma_r$ if distance $|\vec{\psi}^{(t)} - \vec{z}_r|$ is minimum for all positions of the cluster centers. The procedure of k-means minimizes the

sum of squares of all intracluster distances $S(\vec{z}_1, ..., \vec{z}_q) = \sum_{r=1}^{q} \sum_{\vec{\psi}\in\Gamma_r} | \vec{\psi} - \vec{z}_r |^2$ with respect to positions of the cluster centers $\vec{z}_r$.

Let $J(q) = \min_{\vec{z}_1, ..., \vec{z}_q} S(\vec{z}_1, ..., \vec{z}_q)$. We used a test number of clusters in the range of $2 \le q \le 40$. The best number of clusters q^* was determined from the condition of the pseudo-F-statistic (*PFS*) maximum (Vogel and Wong, 1979):

$$PFS(q) = \sigma_1^2(q)/\sigma_0^2(q) \to \max_{2\le q\le 40}, \quad (4)$$

where $\sigma_0^2(q) = J(q)/(L-q)$; $\sigma_1^2(q) = \sum_{r=1}^{q} \nu_r | \vec{z}_r - \vec{z}_0 |^2$; and $\nu_r = n_r/L$, $\vec{z}_0 = \sum_{t=1}^{L} \vec{\psi}^{(t)}/L$.

However, rule (4) is not valid if it is necessary to distinguish the cases $q^* = 1$ and $q^* = 2$, because quantity $\sigma_1^2(q)$ is undefined at $q = 1$. The quantity $\sigma_0^2(q)$ monotonically increases with a decrease in q, and the dependence of $\log(\sigma_0^2(q))$ on $\log(q)$ is usually close to linear, i.e., $\sigma_0^2(q) = q^{-\mu}$. In cluster analysis, the so-called elbow rule is known (Ketchen (Jr.) and Shook, 1996). According to this rule, the optimum number of clusters can be determined by the breakpoint of the function $\sigma_0^2(q)$ for $q = q^*$: with a decrease in q, the quantity $\sigma_0^2(q)$ increases faster for $q < q^*$ than for $q > q^*$. Let $\delta(q)$ denote the deviation of the dependence $\log(\sigma_0^2(q))$ from $\log(q)$ determined by fitting of the linear law: $\log(\sigma_0^2(q)) = b\log(q) + c + \delta(q)$, where coefficients b and c are determined by the least squares method: $\sum_{q=1}^{40} \delta^2(q) \to \min_{b,\ c}$. We assume that the point $q = 2$ is a breakpoint of the dependence $\sigma_0^2(q)$ if $\delta(1)$ exceeds all values $\delta(q)$ for $q \ge 2$.

Let $q_0 = \arg\max_{2\le q\le 40} PFS(q)$. We determine the optimum number of clusters q^* by the following rule (Lyubushin, 2011a, 2013b): if $q_0 > 2$, then $q^* = q_0$; otherwise, if $\delta(1)/\arg\max_{2\le q\le 40} \delta(q) \le 1$, then $q^* = 1$; otherwise, $q^* = 2$.

Figure 2b presents a graph of the evolution of the best number of clusters q^* as a function of the position of the right end of the moving 1-year time window. Figure 2c presents the two-dimensional diagram of $PFS(q)$ as a function of the test number of clusters q and position of the right end of the time window. The diagram is similar in appearance to spectrum-time diagrams. It follows from data presented in Fig. 2b that quantity q^* before the Tohoku megaearthquake of March 11, 2011, exhibited a chaotic regime of changes with jumps from minimum values to maximum ones on a time interval with a length of about 1 year before the event; as is seen in the same figure, this time interval is characterized by higher values of $PFS(q)$. Figure 2d presents the plot of mean values $\bar{P} = \sum_{q=2}^{40} PFS(q)/39$ of the pseudo-F-statistic in each time window, depending on the position of the right end of the window. This dependence exhibits a rather strongly pronounced 2.5-year periodicity established since 2003 with a positive trend of an increase in the mean value of $PFS(q)$. Finally, Fig. 2e depicts the sequence of strong seismic events with a magnitude of no less than 7 in the vicinity of Japanese Islands.

The essence of our hypothesis is that pseudo-F-statistic maps, which are a by-product of the procedure of cluster analysis of multifractal properties and seismic noise entropy in a moving time window, reflect natural fluctuations of seismic hazard in a rather large seismically active region. This hypothesis is based on a comparison of the variation in the quantity *PFS* (Figs. 2c, 2d; curve *1*) and sequence of strong ($M \ge 7$) seismic events (Fig. 2d, lines *2*) in a rectangular vicinity of Japanese Islands (28°–48° N) × (128°–156° E). From the viewpoint of the proposed hypothesis, a regime of natural fluctuations of seismic hazard has been established in Japan since 2003 with a period of about 2.5 years. In particular, the previous cycle of higher values both of q^* and of $PFS(q)$ preceded to the last strong Kumamoto earthquake of April 14, 2016, $M = 7$, in the South of Japan, with the epicenter at 32.78° N, 130.72° E. It follows that 2018 is a year of higher hazard for Japan, because the regime of chaotic fluctuations of q^* has been resumed (see Fig. 2a) and the mean value of the pseudo-F-statistic has begun to grow again (Fig. 2d, curve *1*).

MAPS OF SEISMIC NOISE PROPERTIES

The network of seismic stations covers all of Japan, and one can obtain an estimate of the parameters ($\Delta\alpha$, α^*, $\alpha_{\min}$, *En*) every day from each station. Then, one can construct a daily map of variations in these parameters in space. To obtain a digital map, we cover the rectangular domain, including all the stations, by a uniform mesh of nodes. Then, for each node, we take values of one or another parameter that are equal to the median of the given number of seismic stations closest to the node under consideration. Maps constructed in this way are obtained as a collection of median values of the parameters ($\Delta\alpha$, α^*, $\alpha_{\min}$, *En*) from five stations nearest to each node in nodes of the uniform 30 × 30 mesh covering the rectangular domain with the area 30°–46° N × 128°–146° E.

Averaging daily maps over all days inside a large time interval, we obtain averaged maps.

Such maps are presented in Fig. 3 for three successive time intervals. Among this collection of maps, of greatest interest are maps for values of $\Delta\alpha$ and *En*. As was mentioned in (Lyubushin, 2012a; Lyubushin et al., 2015), waveforms of seismic noise in regions of strong earthquake preparation are characterized by higher values of entropy *En* and lower values of singularity spectrum support width $\Delta\alpha$, which reflects a simpler structure of the noise. Simplification of the seismic-noise structure in strong earthquake preparation zones is presumably associated with processes of small crust blocks of the Earth consolidating into larger ones. As a result of consolidation, high-amplitude spikes, which are a consequence of the mutual motion of small blocks relative to each other, disappear from the waveforms.

In what follows, we mainly comment only the sequence of maps for the distribution of $\Delta\alpha$ (see Fig. 3, (a1)–(a3)), because distribution maps for the entropy *En* (see Fig. 3, (d1)–(d3)) duplicate in antiphase maps for $\Delta\alpha$ to a considerable extent, although there are some differences. The joint use of the quantities $\Delta\alpha$ and *En* is worthwhile, because calculating these quantities is based on quite different approaches.

Figure 3 (a1) presents the distribution map for $\Delta\alpha$ from 1997 (the F-net system getting started) to the strong ($M = 8.3$) event near the coast of Hokkaido Island on September 25, 2003, which was the first strong manifestation of the large-scale growth of lithosphere destabilization in the region of Japan. In some specified sense, this event can be treated as a foreshock (a preliminary shock) of the following megaearthquake.

After the earthquake of 2003, a small but statistically significant decrease in the mean value of $\Delta\alpha$ took place. This is easily seen by comparing maps (a1) and (a2) in Fig. 3. In map (a1), the region of the future megaearthquake is marked by significantly lower values of $\Delta\alpha$, testifying to the beginning of event preparation long before 1997 (introduction of the F-net observation system), which is quite natural because the time of the appearance of the first precursors of megaearthquakes with a magnitude of 9 is estimated at 30–50 years. It is particularly remarkable that the region of lower values of $\Delta\alpha$ decomposed into two parts after the earthquake of 2003 (see Fig. 3 (a2)) and only the northern part was implemented as a region of a megaearthquake.

Figure 3 (a3) shows the spatial distribution of the parameter $\Delta\alpha$ estimated after the Tohoku earthquake (more exactly, during the time interval beginning from March 14, 2011, when the seismic network "recovered itself" after the megaearthquake, to the end of March 2018). It is important to note that, during this time interval, the region containing the hypocenter of the Tohoku earthquake is characterized by higher values of $\Delta\alpha$ (and lower values of entropy) after the seismic catastrophe; i.e., the decomposition of the consolidated state of the Earth's crust and an increase in the number of degrees of freedom took place. An important feature of map (a3) is that the area of relatively low values of $\Delta\alpha$ in the southeast of the region under consideration (the lower right corner of the map) existed before the catastrophe (in 1997–2010) and remained after it. Therefore, following the interpretation of lower values of singularity-spectrum support width $\Delta\alpha$ as an indicator of seismic hazard, we conclude that the region under consideration has been and remains dangerous seismically.

One can suppose that, after the event of September 25, 2003, near the coast of Hokkaido Island, due to the decomposition of the erstwhile consolidated zone of lower values of $\Delta\alpha$ (see Fig. 3 (a1)) into two parts (see Fig. 3 (a2)), a situation in which a strong event could occur both in the northern and in the southern half of the zone was created. Under the influence of different random actions, the northern part was involved and the southern part remained unaffected. It is appropriate to put forward a hypothesis that the Tohoku earthquake relieved only half of accumulated stresses, and the second half waits in the wings. It is the part of the remaining seismic potential that is of serious hazard due to its closeness to the capital of Japan.

It should be noted that this region—the Nankai Trough, where the northern boundary of the Philippine Sea plate approaches the islands of Japan—is considered by Japanese researchers as a place where the most hazardous earthquakes might occur for a long time (Rikitake, 1999; Mogi, 2004). After the Tohoku earthquake, the seismic danger for Japan was revised, and now hypotheses about the possibility of earthquakes with magnitudes of up to 10 in the Japanese oceanic trough are put forward (Zoller et al., 2014). Thus, the multifractal and entropic analysis of seismic noise has yielded an independent estimate of seismic hazard for the region.

Averaged maps (b1)–(b3) and (c1)–(c3) in Fig. 3 for the multifractal parameters α^* and α_{min}, respectively, are of interest in their correlation with maps for $\Delta\alpha$ and *En*. It should be noted that maps of correlations between pairs of parameters $(\alpha^*, \Delta\alpha)$ and (α^*, En) have interesting prognostic properties. By analogy with the maps presented in Fig. 3, one can construct averaged images of the correlation between increments of $(\alpha^*, \Delta\alpha)$. For this purpose, we estimate the evolution of the coefficient of correlation between increments of daily values of $(\alpha^*, \Delta\alpha)$ for each station during a 365-day time window. For each position of the annual time window, one can construct a map by calculating the median of correlation coefficients for five functioning seismic stations nearest to each node of the regular mesh. Averaged maps are created using averaging maps corresponding to all annual time win-

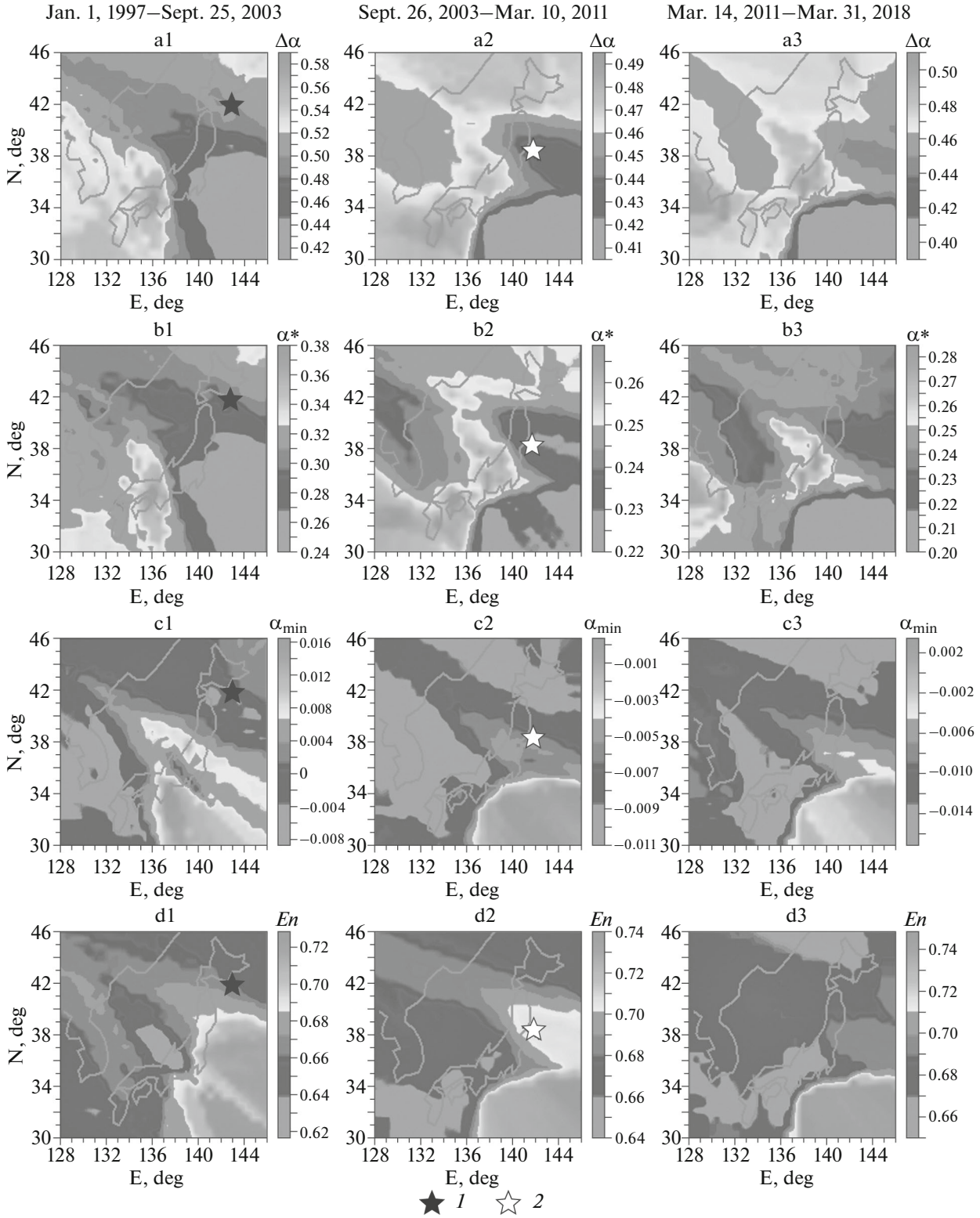

Fig. 3. (a1)–(a3) Averaged maps of the spatial distribution of seismic noise properties: singularity spectrum support width $\Delta\alpha$, (b1)–(b3) generalized Hurst exponent α^*, (c1)–(c3) minimum Hölder–Lipschitz exponent α_{min}, and (d1)–(d3) minimum normalized entropy of squared wavelet coefficients *En* for three time intervals. Epicenters of the earthquakes of (*1*) September 25, 2003, $M = 8.3$, and (*2*) March 11, 2011, $M = 9.1$.

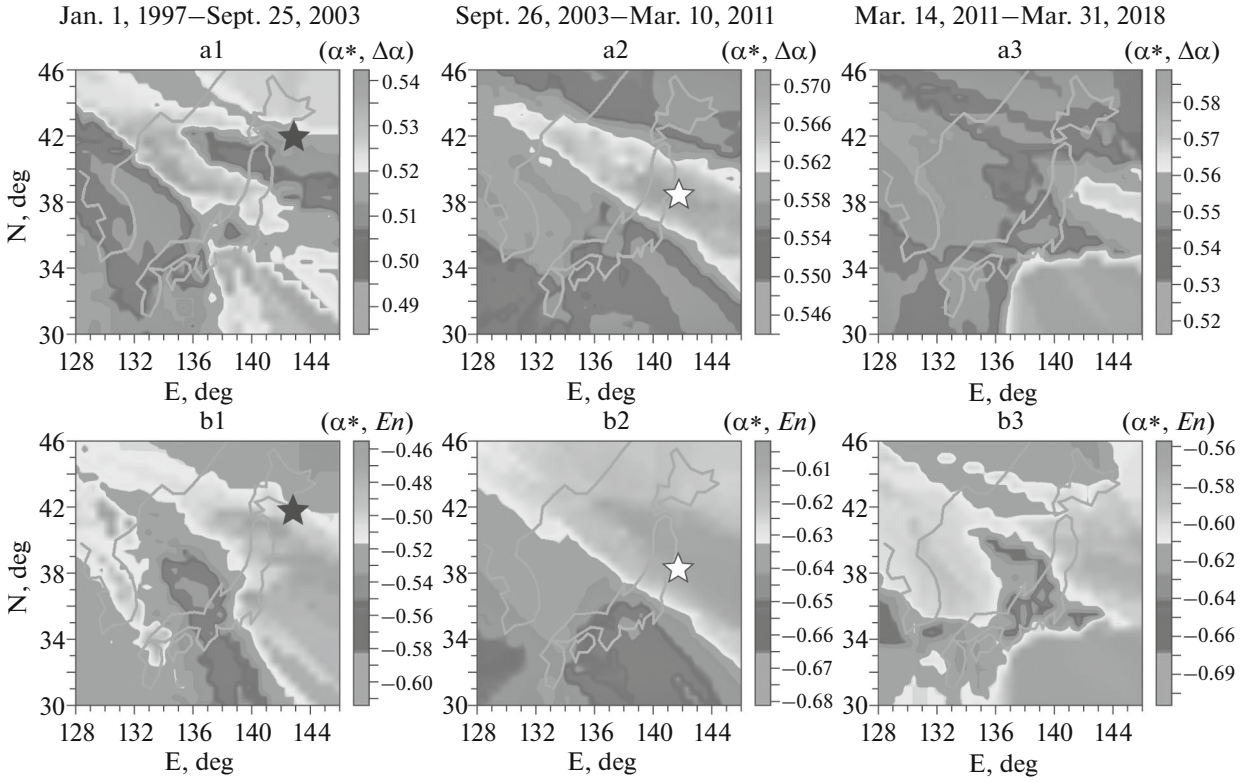

Fig. 4. (a1)–(a3) Averaged maps of the coefficient of correlation between increments of median values of the generalized Hurst exponent α* and singularity spectrum support width Δα. (b1)–(b3) The same for the coefficient of correlation between α* and increments of the minimum normalized entropy of wavelet coefficients *En* for three time intervals. The asterisks mark epicenters of the earthquakes of September 25, 2003, $M = 8.3$, and March 11, 2011, $M = 9.1$.

dows that lie entirely between two dates. Maps of correlation coefficients for pair (α^*, En) can be constructed in a similar way. Such maps are presented in Fig. 4.

It is interesting to note that the region of the future Tohoku earthquake in maps (a2) and (b2) of Fig. 4 is characterized by relatively high absolute values of correlations. Note that the correlations in maps (b1)–(b3) are negative. During the period after the Tohoku earthquake, the region of higher hazard according to Figs. 3 (a3) and (d3) coincided with the region of maximum absolute values of correlations (see Figs. 4 (a3) and (b3)).

MAP OF SEISMIC NOISE CORRELATIONS ACCORDING TO DATA OF GPS STATIONS

The network of seismic observations in Japan is complemented by the dense network of GPS measurements of the Earth's surface motion in three orthogonal directions: East–West (*E*), North–South (*N*), and vertical (*Z*). Currently, the total number of stations for this network is equal to 1341. The arrangement of the GPS stations is shown in Fig. 1. For Japan, three-component time series of the Earth's surface displacements with a step of 5 min are available beginning from March 3, 2015, on the website ftp://gneiss.nbmg.unr.edu/rapids_5min/kenv/. In (Filatov and Lyubushin, 2017a, 2017b), these data were studied using fractal analysis for estimating the current seismic hazard in the Japanese islands.

Let us try to answer the following question: to what extent can an analysis of such high-frequency GPS time series complement the conclusion made (based on an analysis of seismic noise) about the higher seismic hazard in the region of the Nankai Through. For this purpose, we estimate the distribution of the Earth's surface tremor in the correlation space. Just as in Figs. 3 and 4, we use a regular mesh of nodes. Consider a moving 5-day time window, which amounts about 1440 readings at a time step of 5 min. We shift this window by 1 day and find the ten nearest functioning GPS stations for each position of the time window and each node of the regular mesh. Using records of the Earth's surface displacements from these ten stations, we calculate all pairwise correlation coefficients. If the number of nearest stations is equal to 10, there will be 45 correlation coefficients of this kind. Then, we calculate their mean absolute value, which yields a correlation measure related to one or another node of the regular mesh. This measure can take values from 0 to 1. For each position of the moving win-

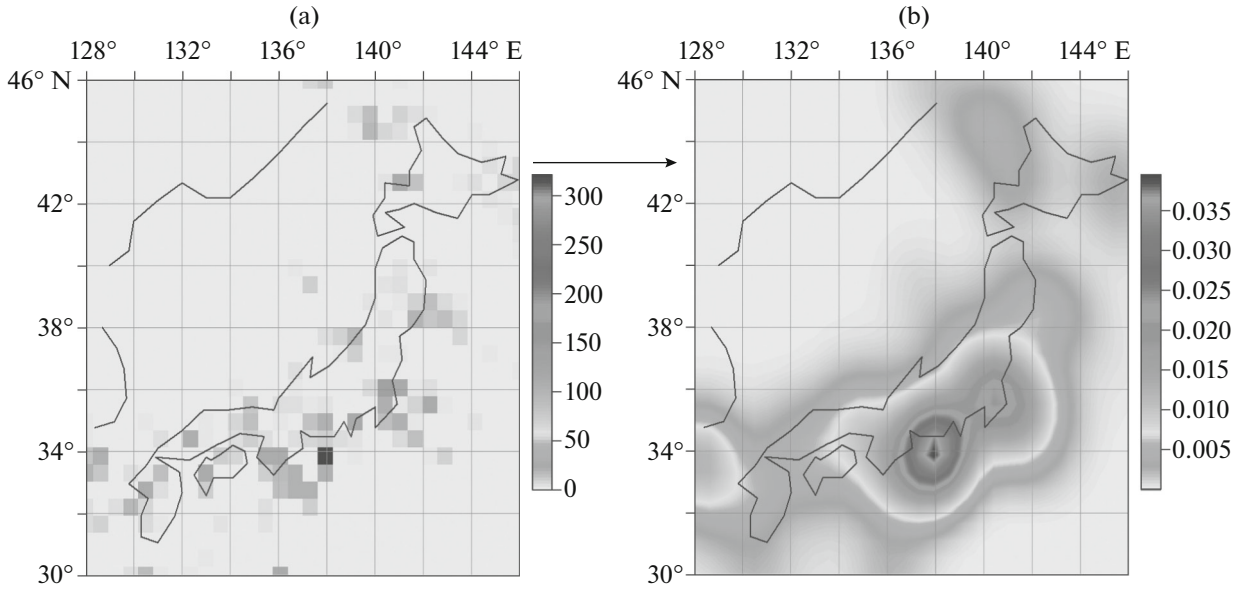

Fig. 5. (a) Two-dimensional histogram of the position of maximums of mean absolute pairwise correlations of time GPS series in Japan from the ten nearest stations in moving 5-day time windows in nodes of the regular grid and (b) two-dimensional probability density of positions of maximums of mean absolute pairwise correlations according to the results of smoothing over the space of the two-dimensional histogram.

dow, we have a 30 × 30-matrix of such values. We find and remember the regular mesh node in which the correlation measure reaches the maximum value among elements of this matrix. Then, we displace the moving time window and repeat the whole procedure.

After the time window passes, all possible positions for all three components of displacements of the Earth's surface (E, N, and Z) and each node of the regular mesh, we have a certain integer of times when the maximum of the mean value of absolute pairwise correlations was implemented in this node. This is a kind of a two-dimensional histogram. In Fig. 5a, such a histogram is depicted for the time interval from March 3, 2015, to March 31, 2018. The histogram can be a source material for the following estimate of the two-dimensional probability density of the distribution of places where the maximum absolute correlation from the ten nearest stations is implemented most often. The estimate of such two-dimensional density is obtained by the spatial smoothing of the histogram by the so-called Gaussian kernel function (Hardle, 1989) with a spatial correlation radius of 1° and following the normalization of the result to make the integral of it equal to 1. The map of such probability density is depicted in Fig. 5b. It is seen that there is a spot with the center at 34° N; 138° E, where the maximum of the average absolute correlation is implemented most often. However, these are coordinates of the center of the Nankai Trough! Thus, the analysis of correlation of high-frequency noises recorded at stations of the GPS network made it possible to more exactly determine the seismic hazard spot in the region where it was determined based on the analysis of seismic noise properties in Figs. 3 and 4.

CONCLUSIONS

Constructing maps of different properties of low-frequency seismic noises (singularity-spectrum support width and minimum normalized entropy of wavelet coefficients) in moving time windows is a new method for estimating the dynamic seismic hazard. This method makes it possible to trace the appearance and evolution of seismic hazard spots. An analysis of the seismic noise detected in Japanese islands by the F-net broadband seismic network made it possible to estimate in advance the approach of the Tohoku megaearthquake of March 11, 2011. According to the analysis of the seismic noise after March 11, 2011, the next megaearthquake may occur in the region of the Nankai Trough in Japan. The time interval of the occurrence of the seismic event can be estimated using the periodic structure of natural fluctuations of seismic hazard with a period of about 2.5 years. An analysis of spatial high-frequency time series of GPS measurements distinguishes a higher noise correlation spot with the center at 34° N, 138° E, which presents an independent estimate of the region of higher seismic hazard in the Nankai Trough.

ACKNOWLEDGMENTS

This work was supported by the Russian Foundation for Basic Research, project no. 18-05-00133.

REFERENCES

Aivazyan, S.A., Bukhshtaber, V.M., Enyukov, I.S., and Meshalkin, L.D., *Prikladnaya statistika: Klassifikatsiya i snizhenie razmernosti* (Applied Statistics: Classification and Dimension Reduction), Moscow: Finansy i statistika, 1989.

Duda, R.O. and Hart, P.E., *Pattern Classification and Scene Analysis*, New York: Wiley and Sons, 1973; Moscow: Mir, 1976.

Feder, J., *Fractals*, New York: Plenum, 1988; Moscow: Mir, 1991.

Filatov, D.M. and Lyubushin, A.A., Assessment of seismic hazard of the Japanese islands based on fractal analysis of GPS time series, *Izv., Phys. Solid Earth*, 2017a, vol. 53, no. 4, pp. 545–555.

Filatov, D.M. and Lyubushin, A.A., Fractal analysis of GPS time series for early detection of disastrous seismic events, *Phys. A (Amsterdam, Neth.)*, 2017b, vol. 469, no. 1, pp. 718–730. http://dx.doi.org/. doi 10.1016/j.physa.2016.11.046

Hardle, W., *Applied Nonparametric Regression*, Cambridge: Cambridge Univ. Press, 1989; Moscow: Mir, 1993.

Huber, P.J., *Robust Statistics*, New York: Wiley, 1981; Moscow: Mir, 1984.

Kantelhardt, J.W., Zschiegner, S.A., Konscienly-Bunde, E., Havlin, S., Bunde, A., and Stanley, H.E., Multifractal detrended fluctuation analysis of nonstationary time series, *Phys. A (Amsterdam, Neth.)*, 2002, vol. 316, pp. 87–114.

Ketchen, D.J., Jr. and Shook, C.L., The application of cluster analysis in strategic management research: An analysis and critique, *Strategic Manage. J.*, 1996, vol. 17, no. 6, pp. 441–458.

Lyubushin, A.A., *Analiz dannykh sistem geofizicheskogo i ekologicheskogo monitoringa* (Analysis of Geophysical and Environmental Monitoring Data), Moscow: Nauka, 2007.

Lyubushin, A.A., Microseismic noise in the low frequency range (periods of 1–300 min): Properties and possible prognostic features, *Izv., Phys. Solid Earth*, 2008, vol. 44, no. 4, pp. 275–290.

Lyubushin, A.A., Synchronization trends and rhythms of multifractal parameters of the field of low-frequency microseisms, *Izv., Phys. Solid Earth*, 2009, vol. 45, no. 5, pp. 381–394.

Lyubushin, A.A., The statistics of the time segments of low-frequency microseisms: trends and synchronization, *Izv., Phys. Solid Earth*, 2010, vol. 46, no. 6, pp. 544–553.

Lyubushin, A.A., Cluster analysis of low-frequency microseismic noise, *Izv., Phys. Solid Earth*, 2011a, vol. 47, no. 6, pp. 488–495.

Lyubushin, A.A., The seismic catastrophe of March 11, 2011, in Japan: Long-term forecast by low-frequency microseisms, *Geofiz. Protsessy Biosfera*, 2011b, vol. 10, no. 1, pp. 9–35.

Lyubushin, A.A., Forecast of the Great Japanese earthquake, *Priroda*, 2012a, no. 8, pp. 23–33.

Lyubushin, A., Prognostic properties of low-frequency seismic noise, *Nat. Sci.*, 2012b, vol. 4, pp. 659–666. doi 10.4236/ns.2012.428087

Lyubushin, A.A., Mapping the properties of low-frequency microseisms for seismic hazard assessment, *Izv., Phys. Solid Earth*, 2013a, vol. 49, no. 1, pp. 9–18.

Lyubushin, A., How soon would the next mega-earthquake occur in Japan?, *Nat. Sci.*, 2013b, vol. 5, no. 8A1, pp. 1–7. doi 10.4236/ns.2013.58A1001

Lyubushin, A.A., Analysis of coherence in global seismic noise for 1997–2012, *Izv., Phys. Solid Earth*, 2014a, vol. 50, no. 3, pp. 325–333.

Lyubushin, A.A., Prognostic properties of random fluctuations in geophysical characteristics, *Biosfera*, 2014b, no. 4, pp. 319–338.

Lyubushin, A.A., Dynamic estimate of seismic danger based on multifractal properties of low-frequency seismic noise, *Nat. Hazards*, 2014c, vol. 70, no. 1, pp. 471–483. doi 10.1007/s11069-013-0823-7

Lyubushin, A.A., Coherence between the fields of low-frequency seismic noise in Japan and California, *Izv., Phys. Solid Earth*, 2016, vol. 52, no. 6, pp. 810–820.

Lyubushin, A.A., Long-range coherence between seismic noise properties in Japan and California before and after Tohoku mega-earthquake, *Acta Geod. Geophys.*, 2017, vol. 52, pp. 467–478. doi 10.1007/s40328-016-0181-5

Lyubushin, A.A. and Sobolev, G.A., Multifractal measures of synchronization of microseismic oscillations in a minute range of periods, *Izv., Phys. Solid Earth*, 2006, vol. 42, no. 9, pp. 734–744.

Lyubushin, A.A., Kopylova, G.N., Kasimova, V.A., and Taranova, L.N., On properties of the field of low-frequency noises recorded on the Kamchatka network of wideband seismic stations, *Vestn. Kamchatskoi Reg. Assots. Uchebno-Nauchnyi Tsentr, Nauki Zemle*, 2015, vol. 2, no. 26, pp. 20–36.

Mallat, S., *A Wavelet Tour of Signal Processing*, San Diego: Academic, 1998; Moscow: Mir, 2005.

Mogi, K., Two grave issues concerning the expected Tokai earthquake, *Earth Planets Space*, 2004, vol. 56, no. 8, pp. li–lxvi.

Rikitake, T., Probability of a great earthquake to recur in the Tokai district, Japan: Reevaluation based on newly-developed paleoseismology, plate tectonics, tsunami study, micro-seismicity and geodetic measurements, *Earth Planets Space*, 1999, vol. 51, pp. 147–157.

Sobolev, G.A., *Kontseptsiya predskazuemosti zemletryasenii na osnove dinamiki seismichnosti pri triggernom vozdeistvii* (The Concept of Earthquake Predictability on the Basis of Seismicity Dynamics in Trigger Influence), Moscow: IFZ RAN, 2011.

Sobolev, G.A., *Seismicheskii shum* (Seismic Noise), Moscow: Nauka i obrazovanie, 2014.

Vogel, M.A. and Wong, A.K.C., PFS clustering method, *IEEE Trans. Pattern Anal. Machine Intell.*, 1979, vol. 1, no. 3, pp. 237–245. doi 10.1109/TPAMI.1979.4766919

Zoller, G., Holschneider, M., Hainzl, S., and Zhuang, J., The largest expected earthquake magnitudes in Japan: The statistical perspective, *Bull. Seismol. Soc. Am.*, 2014, vol. 104, no. 2, pp. 769–779. doi https://doi.org/. doi 10.1785/0120130103

Translated by A. Nikol'skii

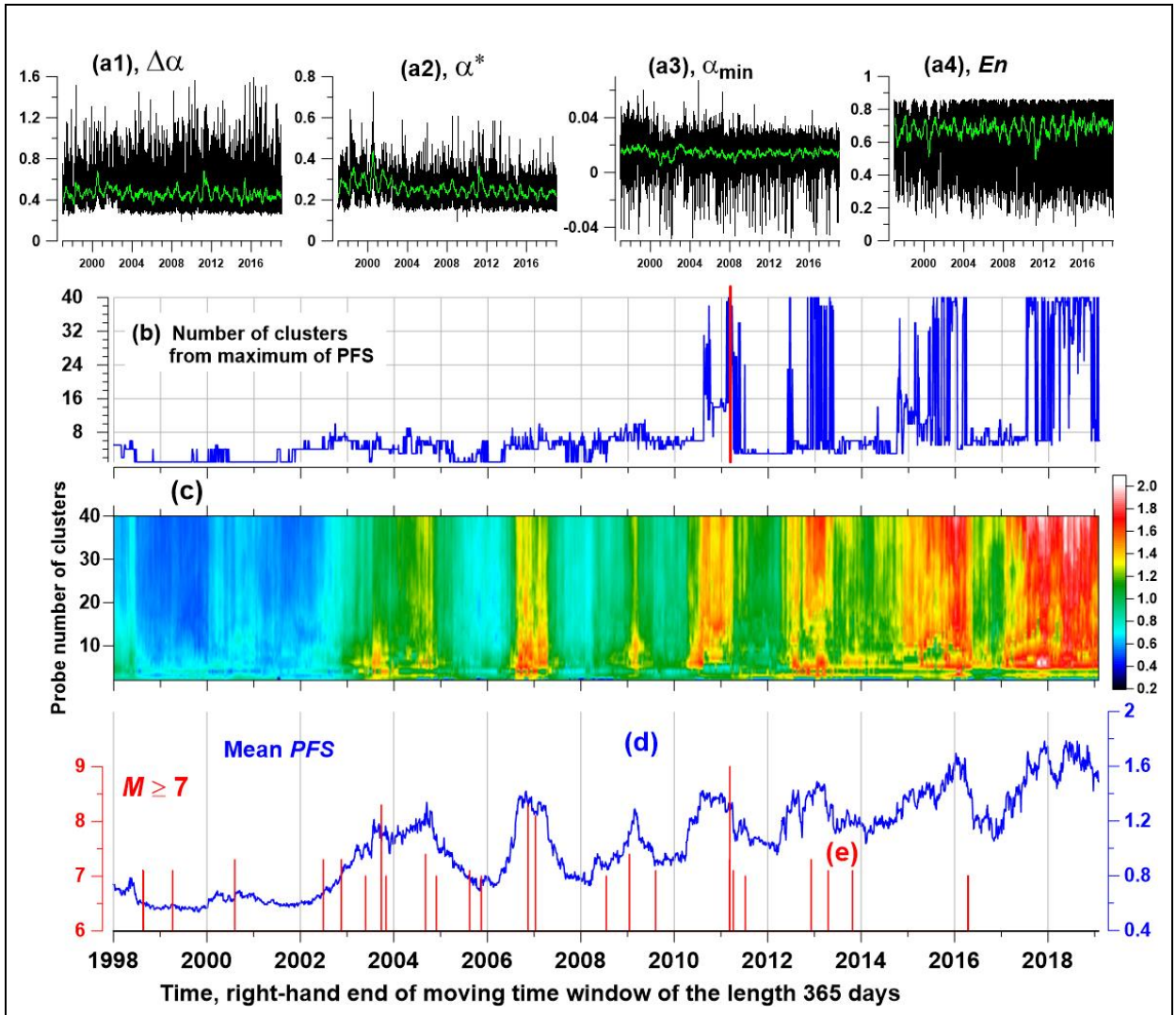

Fig. 2. (a, *black*) Measurement of daily medians of the properties of seismic noise and (*green*) their moving averages in a 57-day window for the interval from January 1, 1997, to January 31, 2019. (b) Best number of clusters as a function of the position of the right end of the moving time window. The vertical red line shows the instant of the mega-earthquake of March 11, 2011. (c) Variability diagram for the quantity *PFS* depending on the position of the right end of the time window and test number of clusters from 2 to 40. (d, *blue*) (*1*) Mean value of the statistic *PFS* as a function of the position of the right end of the time window and (*red*) sequence of seismic events with magnitude $M \geq 7$ in a rectangular region with geographic coordinates (28°–48° N) × (128°–156° E).

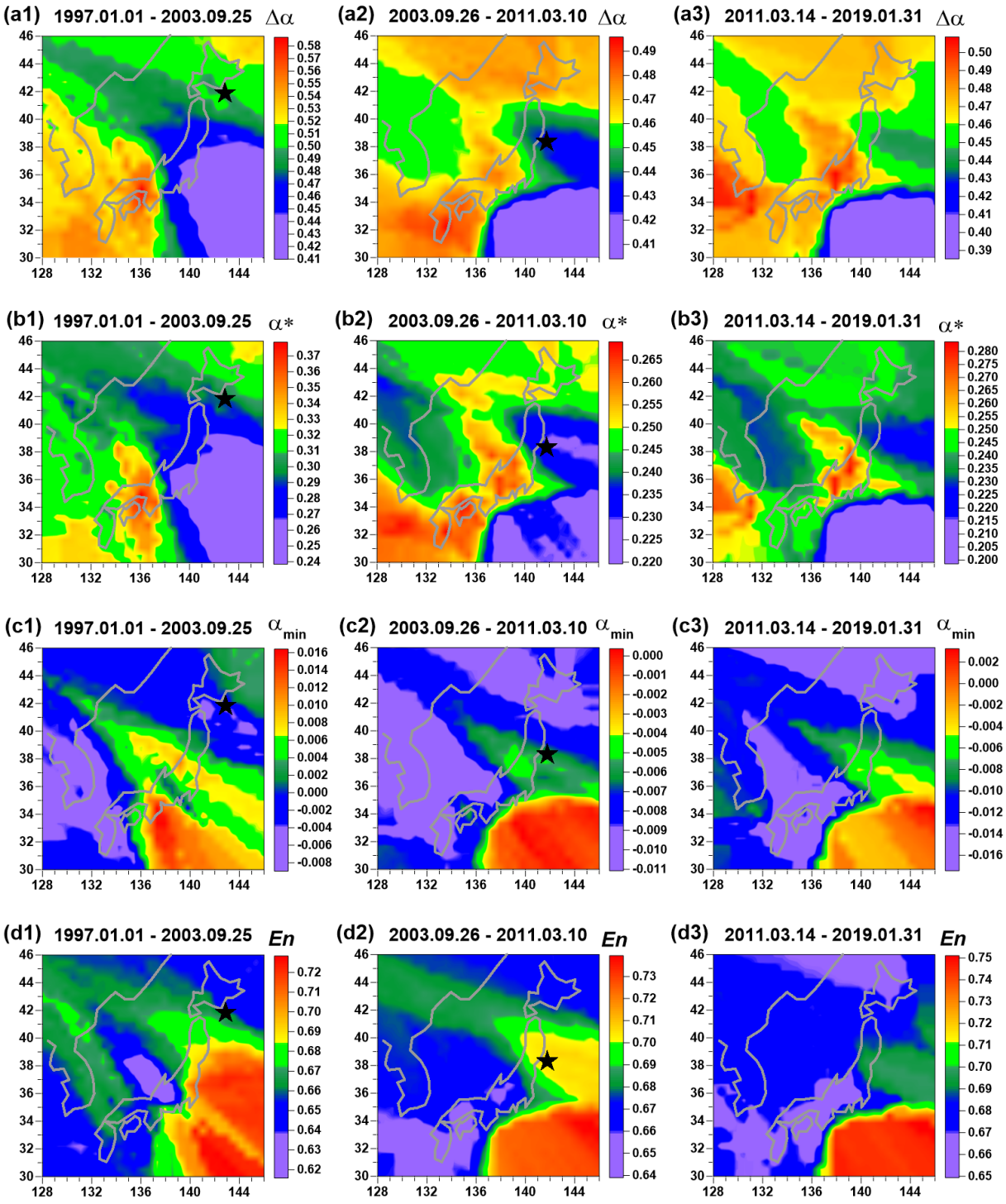

Fig. 3. (a1)–(a3) Averaged maps of the spatial distribution of seismic noise properties: singularity spectrum support width Δα,(b1)–(b3) generalized Hurst exponent α*, (c1)–(c3) minimum Holder—Lipschitz exponent α_{min}, and (d1)–(d3) minimum normalized entropy of squared wavelet coefficients *En* for three time intervals. Black stars - epicenters of the earthquakes of September 25, 2003, *M* = 8.3, and March 11, 2011, *M* = 9.1.

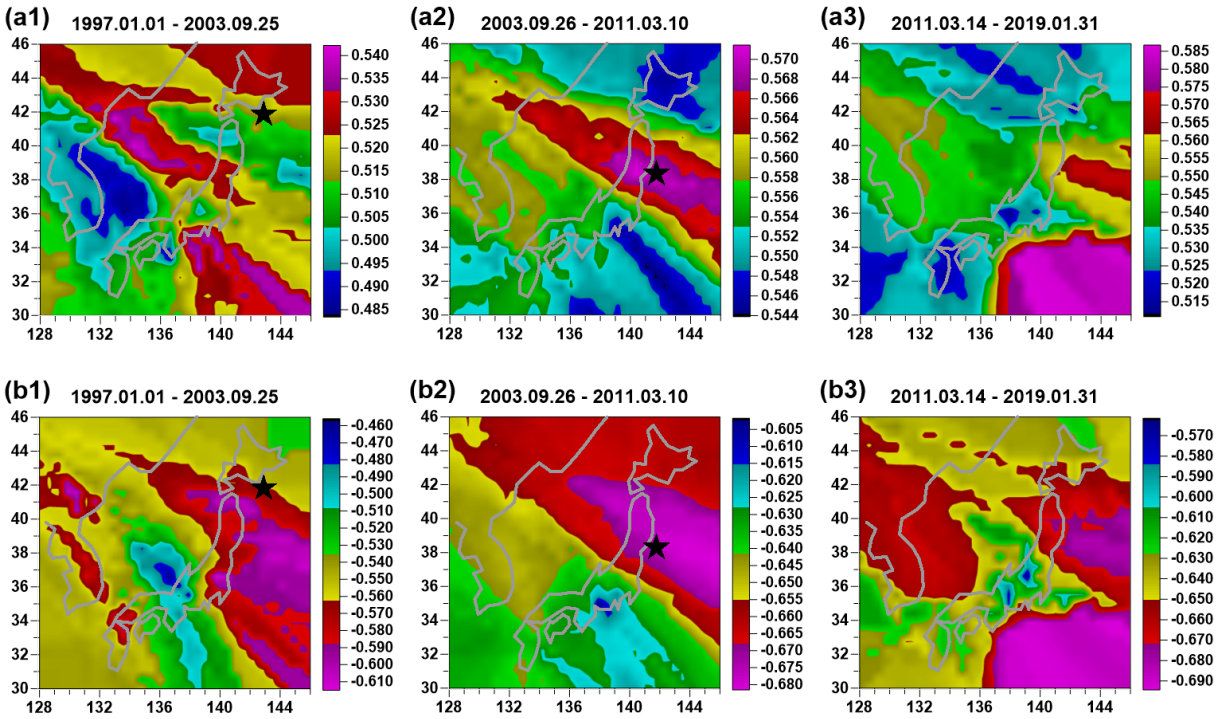

Fig. 4. (a1)–(a3) Averaged maps of the coefficient of correlation between increments of median values of the generalized Hurst exponent α* and singularity spectrum support width Δα. (b1)–(b3) The same for the coefficient of correlation between α* and increments of the minimum normalized entropy of wavelet coefficients *En* for three time intervals. The asterisks mark epicenters of the earthquakes of September 25, 2003, M = 8.3, and March 11, 2011, M = 9.1.

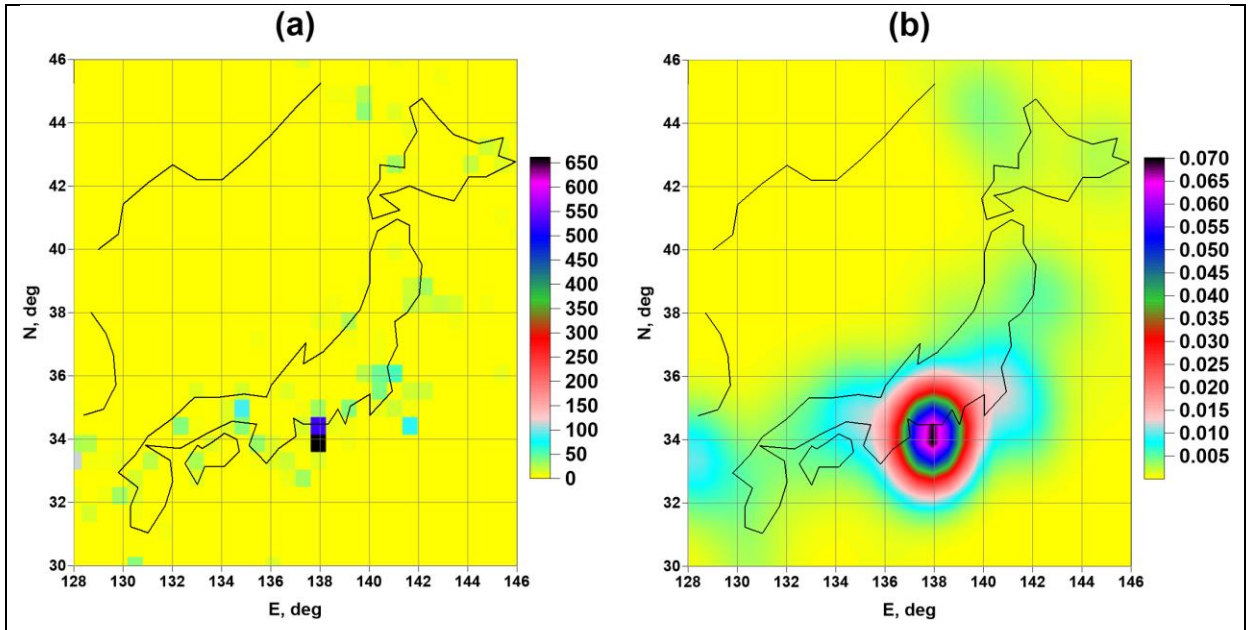

Fig. 5. (a) Two-dimensional histogram of the position of maximums of mean absolute pairwise correlations of time GPS series in Japan from the ten nearest stations in moving 5-day time windows in nodes of the regular grid and (b) two-dimensional probability density of positions of maximums of mean absolute pairwise correlations according to the results of smoothing over the space of the two-dimensional histogram.